Molecular dynamics simulations of highly concentrated salt solutions

Forsyth, M.; Payne, V.A.; Ratner, M.A.; de Leeuw, S.W.; Shriver, D.F.

DOI
10.1063/1.467184
Publication date
1994

Published in
Journal of Chemical Physics

Highly concentrated salt solutions: Molecular dynamics simulations of structure and transport

V. A. Payne, M. Forsyth,[a] M. A. Ratner,[b] and D. F. Shriver
Department of Chemistry and Materials Research Center, Northwestern University, Evanston, Illinois 60208

S. W. de Leeuw
Laboratory for Physical Chemistry, Nieuwe Achtergracht 127, 1018 WS Amsterdam, The Netherlands and Department of Computer Science, Coates Hall, Louisiana State University, Baton Rouge, Louisiana 70803

(Received 28 January 1993; accepted 21 December 1993)

Molecular dynamics (MD) simulations in NaI solutions, where the solvent has been represented by the Stockmayer fluid, were performed as a function of temperature, salt concentration, and solvent dipole strength. At higher temperatures contact ion pairs become more prevalent, regardless of solvent strength. An examination of the temperature dependence of the potential of mean force demonstrates the entropic nature of this effect. The transport properties calculated in the simulations are dependent on the balance between solvent dielectric constant and ion charge. In systems with a large solvent dipole moment, the ions appear to be independently mobile, and deviations from Nernst–Einstein behavior are small. In systems of smaller solvent dipole moment or greater ion charge, the ions form clusters, and large deviations from Nernst–Einstein behavior are observed.

I. INTRODUCTION

Solid polymer electrolytes with no volatile components[1] are fundamentally different from conventional liquid[2–4] or solid electrolytes.[5] The charge carriers originate in a salt that has been solvated by polar groups on the backbone or side chains of the polymer. The behavior of the equivalent ionic conductivity as a function of concentration of salts dissolved in poly (ethylene oxide) (PEO) is typical of these materials: A rather broad minimum is found in the range 0.01–0.1 mol kg^{-1}, followed by increasing equivalent conductivity at higher concentrations.[6–8] These observations are clear evidence for some type of ion pairing or clustering, but the literature has been divided on the structural details.

One explanation suggests that the conductivity minimum is due to the formation of nonconductive ion pairs. Larger ion clusters which can transport charge are formed at higher salt concentrations. Vincent and co-workers[7] suggest that no free ions could exist in such concentrated solutions, so the charge carriers must be aggregates of at least three ions. An alternative explanation of the conductivity dependence on salt concentration holds that, at the higher concentrations, locally free ions are formed from the dissociation of pairs and clusters. This explanation is often seen for the conductivity minimum observed in other electrolytes.[8–10] Cheradame[11] suggested that free ions are the major charge carrier, and that more free ions should be available at higher temperature; he considered the release of free carriers to be an activated phenomenon in which temperature overcomes the binding energy E_B holding the ion to a pair or cluster.

Support for the free-ion mobility picture has been provided by pulsed field gradient NMR experiments to measure cation and anion diffusion coefficients in PEO/salt complexes well above the melting point of PEO.[6] If the charge is carried by free ions, the system will exhibit Nernst–Einstein behavior, and the conductivity coefficient can be directly related to the measured diffusion coefficients. The system exhibited behavior near to the Nernst–Einstein prediction for very high salt concentrations (2–4 mol kg^{-1}) and lower temperatures. The authors hypothesize that equilibrium in these systems consists of large ion clusters similar to those in molten salts. Cooperative configurational rearrangements of these clusters lead to transitory single ions that conduct the charge.

Vibrational spectroscopy has been an extensively used technique for the study of ion pairing in liquid and polymer electrolytes.[12–19] Torell[12] and Frech[19] and their co-workers have observed increased ion association with higher temperature. It has been postulated that the dissolved ions act as "virtual" crosslinks that decrease the entropy of the polymer. Schantz[13] has analyzed the Raman experiments on uni-univalent salts in poly (propylene oxides), and concludes that the simple pairing reaction, written formally as $M^+ + X^- \rightarrow MX$ exhibits large positive entropy change ($T\Delta S° = 36 \pm 12$ kJ/mol for $LiClO_4$), which dominates a small positive enthalpy change to make the pairing thermodynamically favored. Nitzan and Ratner[20] have formalized this explanation in terms of solvent configurational degrees of freedom. More recently, Olender and Nitzan[21] have used mean-field models to analyze ion solvation and desolvation in macromolecular fluids. A microscopic picture is still lacking on the exact nature of ion–ion and ion–solvent interactions in polymer electrolytes.

Useful insights into the structure and dynamics of both dilute[21–23] and more concentrated aqueous solutions[24,25] have been derived from MD and Monte Carlo approaches. Jorgensen *et al.*[22] have extensively investigated the energetics of hydration for dilute concentrations of alkyl and alkyl ammonium chloride salts. McCammon *et al.*[23] have calculated both the solvation structure and the dynamics of a sodium

[a]Permanent address: Department of Materials Engineering, Monash University, Wellington Road, Clayton, Victoria 3168, Australia.
[b]Author to whom correspondence should be addressed.

 0021-9606/94/100(7)/5201/10/$6.00

TABLE I. Physical parameters used in simulations.

Particles	σ (Å)	ϵ (K)	$z(e)$	μ (D)	mass (amu)	Moment of inertia I
Na	1.9	58.2	$+\frac{1}{2}$; $+1$	0	23	...
I	4.2	420	$-\frac{1}{2}$; -1	0	126.9	...
Solvent	3.07	90	0	1.3; 2	44	0.05

chloride pair in water. Both groups of investigators have found two minima in the potential of mean force corresponding to a contact ion pair and solvent-separated ion pair for unlike ions. Also, the frequency-dependent behavior of the conductivity of a model electrolyte solution has been studied by MD.[26] Ciccotti *et al.*[27] investigated ionic transport in molten alkali halides and have achieved good agreement with experimentally measured properties.

Developments based on solution of the Ornstein–Zernike equation using a number of differing physical models and formal closures have been extended to quite high concentrations, and have yielded important general structural insights on ionic solutions.[28–30] In particular, failure of the primitive model in predicting the potentials of mean force has been explained in terms of overscreening at short separations, and failure to account for the true solvent structure, in which solvent molecules occupy physical space (producing, e.g., solvent-separated pairs). MD and MC[31–33] simulations have been of real value both for comparison with the analytical developments and for investigating some properties, such as cluster shapes, that are more difficult to get from the Ornstein–Zernike solutions.

The present manuscript examines the fundamental interactions in models for polymer electrolytes through the use of MD simulations. The polymer solvent is represented by Stockmayer particles, which are Lennard-Jones spheres containing a point dipole. Although this is not a realistic description for a large, structured solvent such as a polymer, it does allow study of ion behavior in a system with a solvent dielectric constant close to that of the solvent in a polymer electrolyte. Studies using quite different approaches have been started in other groups.[34]

This work studies the effects of temperature, solvent dielectric constant, and ion concentration on the interactions between ions and solvent particles. Both structural and transport properties are investigated. The transport properties of the system are studied by calculating diffusion and conductivity coefficients and comparing the behavior of the system to predictions of Nernst–Einstein behavior. The thermodynamic properties of the system are investigated through the calculation of the potential of mean force, the free energy of a particle pair as a function of separation distance. The temperature dependence of this function allows determination of the entropic and energetic contributions to the stability of contact and solvent-separated ion pairs. We demonstrate that greater ion association with higher temperature is essentially an entropic effect.

II. COMPUTATIONAL DETAILS

MD simulations were carried out on a system consisting of NZ ions and ND solvent molecules at fixed temperature and volume. The particle parameters given in Table I approximate a system of NaI dissolved in an ether solvent.[35] The potential energy of the system, taking into account Lennard-Jones (LJ), dipole–dipole (DD), ion–dipole (iD), and ion–ion (Coul) interactions, is given by Eq. (1):

$$\begin{aligned} V(\mathbf{R}_1,\ldots,\mathbf{R}_n,\boldsymbol{\mu}_1,\ldots,\boldsymbol{\mu}_{\mathrm{ND}},Z_1,\ldots,Z_{\mathrm{NZ}}) &= \frac{1}{2}\sum_{i=1}^{(\mathrm{ND}+\mathrm{NZ})}\sum_{j\neq i}^{(\mathrm{ND}+\mathrm{NZ})}\phi_{\mathrm{LJ}}(|\mathbf{R}_{ij}|) \\ &+\frac{1}{2}\sum_{i=1}^{\mathrm{ND}}\sum_{j\neq i}^{\mathrm{ND}}\phi_{\mathrm{DD}}(\mathbf{R}_{ij},\boldsymbol{\mu}_i,\boldsymbol{\mu}_j) \\ &+\sum_{i=1}^{\mathrm{NZ}}\sum_{j=1}^{\mathrm{ND}}\phi_{\mathrm{ID}}(\mathbf{R}_{ij},Z_i,\boldsymbol{\mu}_j) \\ &+\frac{1}{2}\sum_{i=1}^{\mathrm{NZ}}\sum_{j\neq i}^{\mathrm{NZ}}\phi_{\mathrm{Coul}}(|\mathbf{R}_{ij}|,Z_i,Z_j). \end{aligned} \tag{1}$$

The Ewald sum was used to evaluate the long-range coulombic interactions using "tinfoil" boundary conditions.[36] The real space part was truncated at half the box length L and the convergence parameter in the Fourier space sum was taken as $6.58/L$. The reciprocal lattice sum included all vectors for which $[k]^2<27/L^2$. The temperature of the system was held constant with a Nosé heat bath.[37] Reduced units were employed in the algorithm, thus all lengths are measured in units of the Lennard-Jones size parameter for the solvent σ_c and all energies are calculated in units of the LJ well depth of the solvent ϵ_c. The reduced temperature is defined as $T^*=k_BT/\epsilon_c$ and the unit of time is given by

$$\tau=(m_c\sigma_c^2/\epsilon_c)^{1/2}.$$

A reduced density of $\rho^*=1$ was used throughout. This is equivalent to a real density of 2.7 g/cm^3. Some simulations were also repeated with $\rho^*=0.5$ for comparison. In these latter simulations the pressure was found to drop considerably with decreasing temperature and become negative at $T^*=2$ whereas at a reduced density of 1, the reduced pressure was maintained at about 5.5. Simulations were run with 256 particles, however, the number dependence of the results was tested by carrying out simulations with 500 and 1098 particles. The structural results appeared to be independent of box size, however there were some differences in the transport properties, probably as a result of the shorter simulation times necessitated by the computational time required for the larger samples. This resulted in greater uncertainty in the calculated conductivities and diffusion coefficients.

Table II summarizes the computer experiments that will be discussed. The dielectric constant ϵ was calculated in our systems using the Kirkwood formula[37] with tinfoil boundary conditions, $\epsilon=1+3yg$ where $y=4\pi\rho_0\mu^2/9kT$, μ=dipole moment, ρ_0=solvent density, and $g=\langle\mathbf{M}^2\rangle/ND\boldsymbol{\mu}^2$. $\langle M^2\rangle$ is calculated throughout the simulation using $\mathbf{M}=\sum_i^{\mathrm{ND}}\boldsymbol{\mu}_i$.

TABLE II. Systems studied by simulation.

Simulation	No. of solvent molecules	No. of ion pairs	Conc. (M)	T^*	ρ^*	μ (D)	$\lvert z\rvert$ (e)	Time steps
A	240	8	1.8	2, 3, 3.5, 5	1	1.3	$\frac{1}{2}$	100 000
B	240	8	1.8	2, 3, 4	1	1.3	1	100 000
C	224	16	3.6	3, 4	1	1.3	1	100 000
D	248	4	0.9	4	1	1.3	1	100 000
E	232	12	2.7	4	1	1.3	1	100 000
F[a]	240	8	1.8	2, 3, 4	1	2	1	20 000
G	484	8	0.9	3	1	1.3	1	40 000

[a]Only static properties were obtained.

This form can be used to estimate the dielectric constant contribution from the solvent even for a conductive system, where the overall $\epsilon(\omega=0)$ is not measurable. The potential of mean force was calculated from the simulation using 8 ion pairs and 240 solvent molecules.[38]

III. STRUCTURAL PROPERTIES

The cation–solvent and cation–anion radial distribution functions (rdfs) obtained from simulations A, B, C, and F are shown in Figs. 1–4. Each figure also shows the total number of particles of species b within a given distance from a given particle of species a for the rdf $g_{ab}(r)$. The particle number $N_{ab}(r')$ can be obtained from the equation

$$N_{ab}(r')=4\pi\rho_b\int_0^{r'} g_{ab}(r)r^2\,dr, \tag{2}$$

where ρ_b is the number density of species b.

Figure 1 shows two peaks in the Na–I rdf at $r=0.9$ and $r=1.9$, which correspond to contact ion pairs and solvent-separated ion pairs, respectively. A moderate increase in pair-

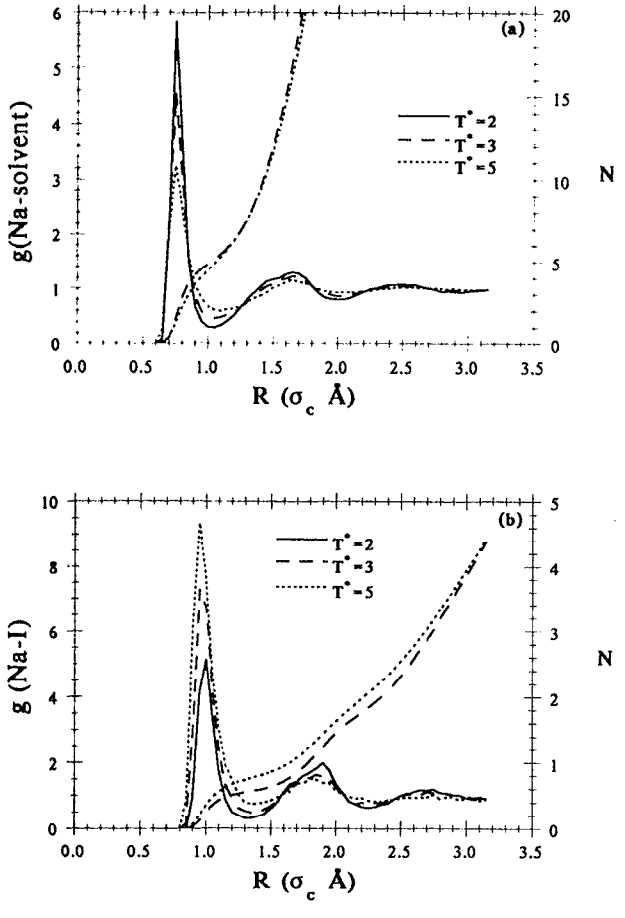

FIG. 1. Cation–solvent and cation–anion radial distribution functions and integrations as a function of temperature [$T^*=2$ (180 K), $T^*=3$ (270 K), $T^*=5$ (450 K)] in experiment A; 8 ion pairs, 240 solvent molecules, $\mu=1.3$ D, $\rho^*=1$, and $z=\frac{1}{2}e$. Distances are scaled by the Lennard-Jones parameter of the solvent $\sigma_c=3.07$ Å. The relatively larger noise level for the ion–ion curves is due to fewer particles, hence to poorer statistics.

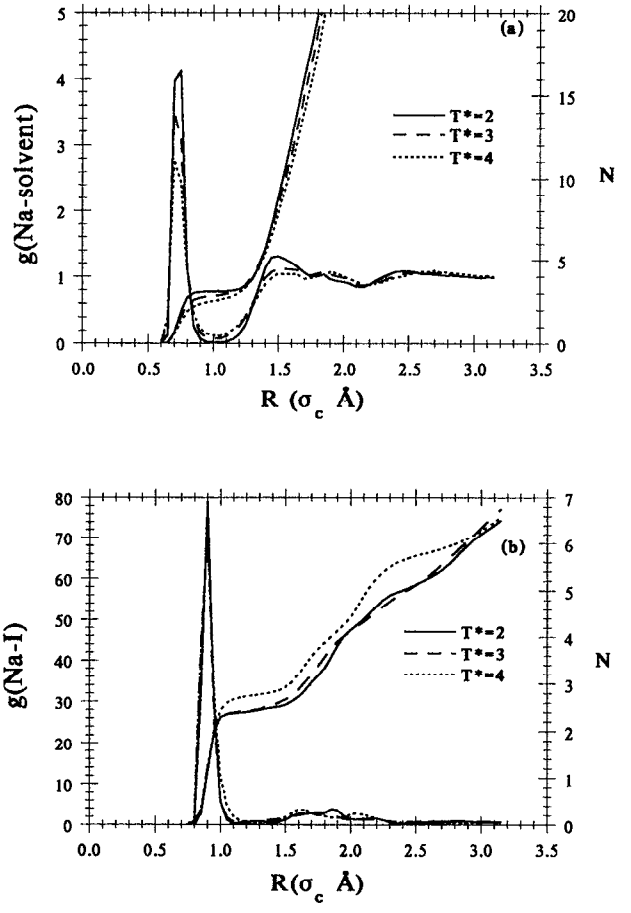

FIG. 2. Radial distribution functions and integrations as a function of temperature [$T^*=2$ (180 K), $T^*=3$ (270 K), $T^*=4$ (360 K)] in experiment B; 8 ion pairs, 240 solvent molecules, $\mu=1.3$ D, $\rho^*=1$, and $z=1e$.

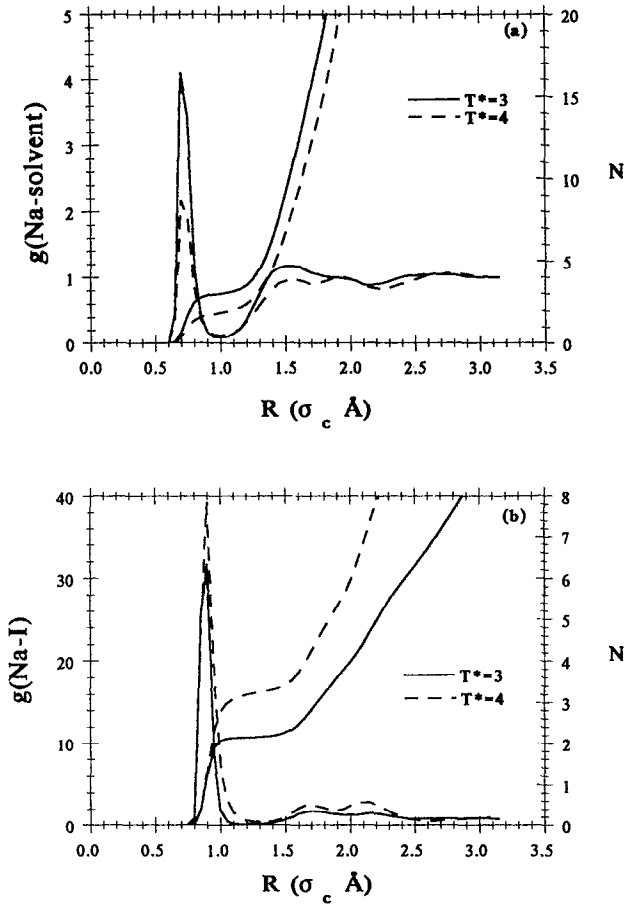

FIG. 3. Radial distribution functions and integrations as a function of temperature [($T^*=3$ (270 K), $T^*=4$ (360 K)] in experiment C; 16 ion pairs, 224 solvent molecules, $\mu=1.3$ D, $\rho^*=1$, $z=1e$.

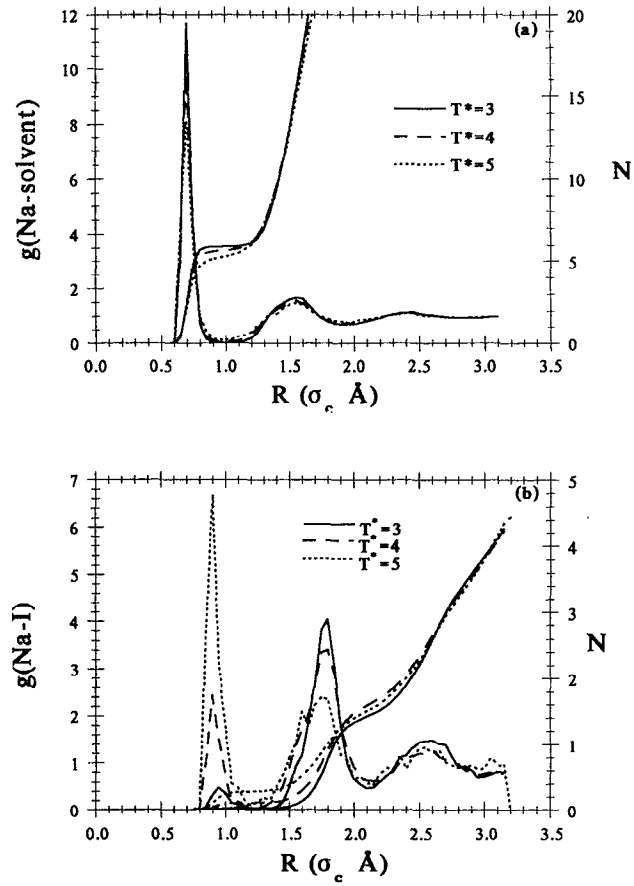

FIG. 4. Radial distribution functions and integrations as a function of temperature [$T^*=2$ (180 K), $T^*=3$ (270 K), $T^*=4$ (360 K)] in experiment F; 8 ion pairs, 240 solvent molecules, $\mu=2$ D, $\rho^*=1$, and $z=1e$.

ing is observed with higher temperature for this system with ion charge $z=1/2$. Figure 2 shows the results for an ion charge of $z=1$. A doubled charge doubles the relative strength of ion–ion interactions as compared to ion–solvent interactions. The Na–I rdf in Fig. 2 shows little change with temperature, unlike Fig. 1. Ion clustering is observed at all temperatures for the $z=1$ system. On average, each cation appears to coordinate with two to three (dependent on temperature) solvent particles and two to three anions. The increase in ion clustering with greater charge could clearly be seen by examination of visual snapshots.

Figure 3 shows the effect of greater ion concentration on the system with $z=1$ and solvent dipole moment $\mu=1.3$ D. The Na–I rdf shows a stronger temperature effect than in the less concentrated system of Fig. 2. Ion association is seen to increase with higher temperature. The anion coordination of the cation appears to increase by one as the temperature increases from 270 to 360 K. Visual snapshots have indicated that phase separation occurs at the higher temperature.

Figure 4 shows the rdfs from the system in which the solvent dipole moment was increased to $\mu=2$ D. At $T=270$ K, the dielectric constant for this solvent was determined to be 80. At all temperatures, ions show significant interaction with the solvent, and no clustering is visible at the lowest temperature. As the temperature is raised, however, some degree of increased ion association occurs, with the Na–I rdf showing an increase in the contact ion pair peak and a corresponding decrease in the solvent-separated peak.

As discussed previously, the apparent increased ion association with increasing temperature has several possible explanations. This effect is not unique to polymer solvents, but may be found in a variety of other solvent systems. Smid and co-workers have observed increased ion pairing with increase in temperature in a number of studies in simple ether solutions, as well as polymer electrolytes.[39,40] Solubility trends show similar behavior: for instance, for NaI in 2-butanone. At first the solubility increases, but at higher temperatures a substantial decrease in solubility can be seen.[41] One part of the explanation must be that the dielectric constant (ϵ) of solvents tends to decrease with increasing temperature. Figure 5 shows ϵ calculated under various simulation conditions, and an inverse temperature dependence can be seen. With decreased dielectric screening, the effective interaction among ions will increase, and more ion association will occur.

However, this explanation is unlikely to be the sole cause of the temperature effect. The postulated decrease in entropy of polymers from loss of low-frequency modes due to ion interactions[20] can also apply to simpler solvents. The

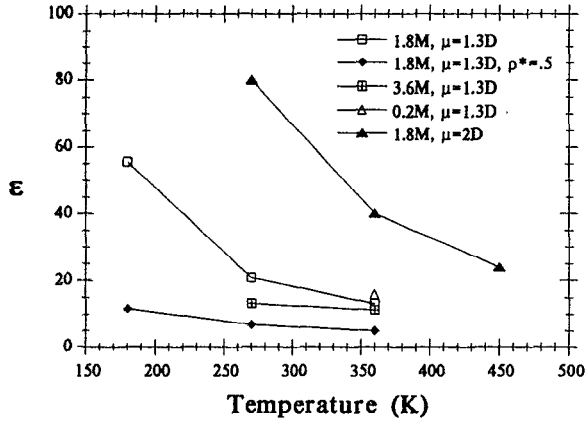

FIG. 5. Calculated static dielectric constant as a function of temperature, salt concentration, and dipole moment.

ions in a polar solvent add structure by causing the dipoles to orient themselves through ion–dipole forces. When two ions pair, they form a dipolar unit which interacts with solvent dipoles through dipole–dipole forces. The weaker forces order the solvent less effectively.[42] Thus ion pairing or clustering leads to an increase in entropy for the entire system. In Sec. IV, evidence will be presented to support the idea that increase in ion association with greater temperature is largely an entropic effect.

IV. THERMODYNAMIC PROPERTIES

The issue of whether the driving force for ion pairing is dominantly entropic or energetic can be clarified by examining the temperature dependence of the potential of mean force (pmf). If we define the standard state for free energy as that for infinitely separated cation and anion, then we can write

$$dA = d(U - TS), \tag{3}$$

$$A - A^{(0)} = U - U^{(0)} - T(S - S^{(0)}). \tag{4}$$

Thus defining

$$A^{(0)} = A(r \to \infty) \equiv 0, \tag{5}$$

we have

$$-\left(\frac{\partial A}{\partial T}\right)_v = (S - S^0), \tag{6}$$

$$A - T\left(\frac{\partial A}{\partial T}\right)_v = U - U^{(0)}. \tag{7}$$

Therefore, if we identify the free energy with the potential of mean force via

$$g(r) = \exp\{-W(r)/k_B T\}, \tag{8}$$

$$A = W(r). \tag{9}$$

[This definition is consistent with Eq. (5), since $g(r \to \infty) = 1$.) Then calculation of $W(r)$, $\partial W(r)/\partial T/_v$ yields $U - U^{(0)}$ and $S - S^{(0)}$. These are plotted in Figs. 6 and 7.

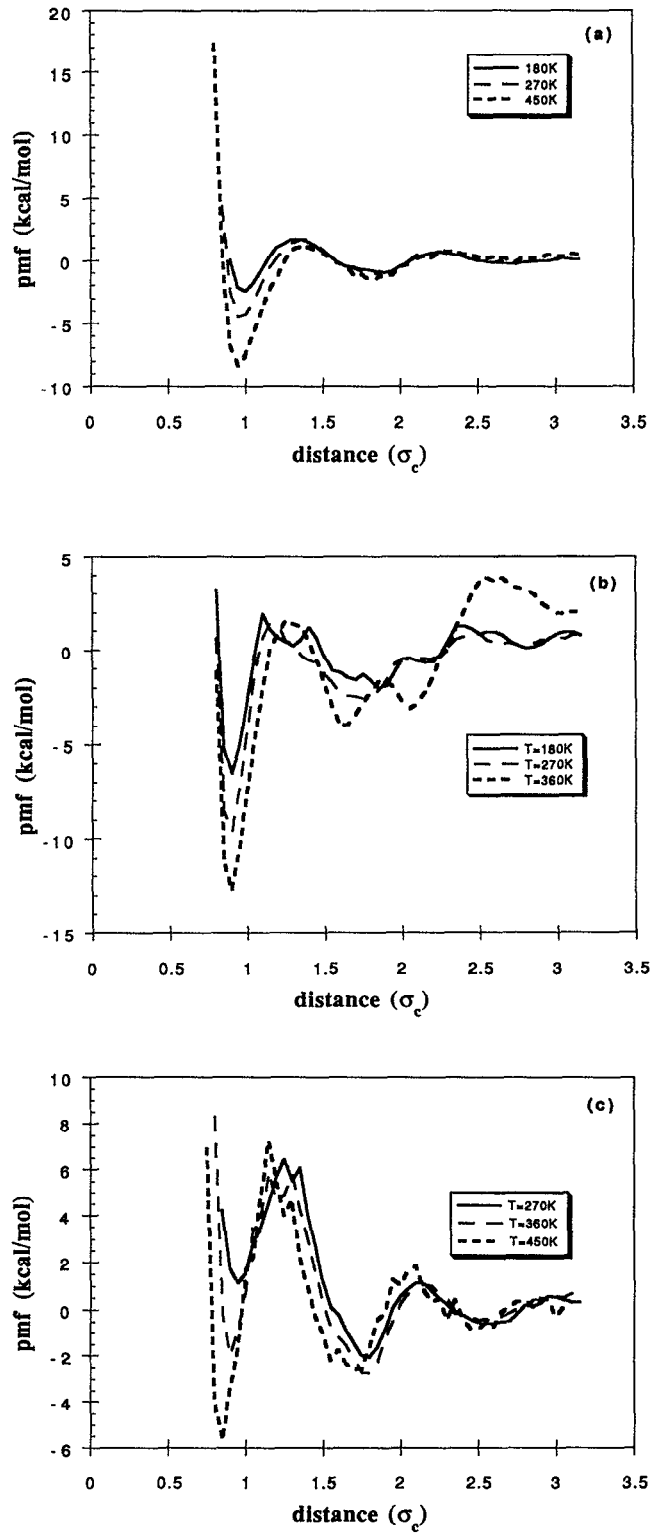

FIG. 6. Potential of mean force for Na–I pairs as a function of temperature; (a) $z = \frac{1}{2}e$, $\mu = 1.3$ D; (b) $z = 1e$, $\mu = 1.3$ D; (c) $z = 1e$, $\mu = 2$ D. Calculated from the pair distribution function g_{NaI} for systems with eight ion pairs.

The potential of mean force was also determined for a single ion pair, Na–I, by calculating the Helmholtz free energy as a function of interionic separation. This was achieved by calculating the free energy of charging the ion pair in the Stockmayer fluid and the energy required to separate an un-

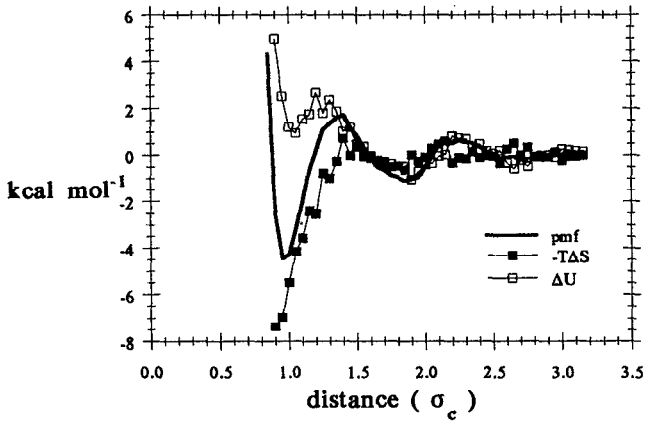

FIG. 7. Thermodynamic decomposition of the potential of mean force for eight NaI pairs calculated from the temperature dependence of the pmf (Fig. 6) at $T=270$ K, $z=0.5e$, $\mu=1.3$ D.

charged pair. The free energies calculated from the simulations were zeroed by comparison with the primitive model prediction at an interionic separation of 7.4 Å. The primitive model potential is calculated from the sum of the Lennard-Jones potentials between the ion pair and the coulombic interaction divided by the calculated dielectric constant.

The pmfs for several temperatures from simulations A, B, and F are shown in Fig. 6. The system where $z=1/2$ [Fig. 6(a)] shows two minima at distances corresponding to contact ion pairs and solvent-separated ion pairs. When the charge is increased to $z=1$ as in Fig. 6(b), the minimum for the contact ion pair deepens, and the solvent-separated pair minimum is replaced by two minima at positions expected for sites on a cubic closest-packed lattice, which agrees with the findings discussed in Sec. III for the rdfs. When the solvent dipole moment is increased to $\mu=2$ D, as in the system of Fig. 6(c), the contact pair minimum (+1 kcal/mol) becomes less favorable at 270 K than that of the solvent-separated pair (−2 kcal/mol). Both minima occur at shorter distances as the temperature increases. The contact pair increases in stability with higher temperature. The pmf of the contact pair at 450 K has dropped to −5.5 kcal/mol. At all temperatures a shallow third minimum is visible at longer distances, probably due to a second solvation sphere for the ions.

The analysis discussed in Eqs. (3)–(9) was performed to separate the energetic and entropic contributions to the Na–I pmf. Figure 7 shows the results for system *A*. Energetic considerations militate against squeezing ions below the Lennard-Jones contact distance. As the distance is subsequently increased, energy appears to weakly favor the formation of contact ion pairs, while the entropy gain is the driving force for contact pairs. Figure 8 shows the pmfs calculated for a single Na–I pair in a box with 256 solvent particles for two different temperatures. It is still possible to distinguish a minimum for a contact ion pair and one for a solvent-separated pair, so the pair must spend some time in each of these states. The second minimum is deeper in the case of the higher solvent dipole moment. The predictions of the primitive model, which treats the solvent as a dielectric continuum without individual particles,[22,43] are also shown in Fig. 8. The primitive model is observed to be inadequate for describing the system structure, particularly the solvent-separated pair. The increased depth of the contact pair minimum is accounted for by the primitive model, since it does include reduced dielectric screening at higher temperatures.

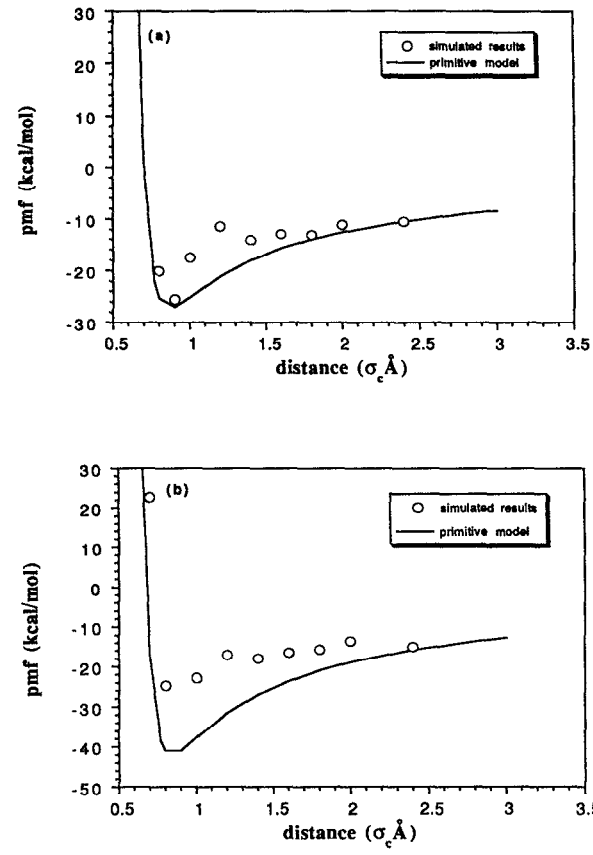

FIG. 8. Potential of mean force for a single Na–I pair in a Stockmayer fluid with (a) $\mu=1.3$ D, $T=270$ K; (b) $\mu=1.3$ D, $T=360$ K. The primitive description does not predict the barrier to formation of a solvent-separated ion pair.

Some evidence has been offered here to support the postulate that even in a simple spherical solvent, entropic considerations are sufficient to explain increased ion association with increasing temperature. These results are in qualitative agreement with analytical calculations for sodium chloride in water by Pettitt and Rossky,[43] who also conclude ion pairing is entropy driven. After taking into account the temperature, charge, and particle size differences between this work and their work, it seems clear that the entropy contribution favoring contact ion pairs is at least twice as large in the Stockmayer fluid as compared to water. The more structured solvent with the large dielectric constant is less easily affected by the ions. No literature source was located which had a thermodynamic decomposition of the potential of mean force for an alkali iodide at any concentration.

In a spectroscopic study of $LiNO_3$ in dimethyl sulfoxide, Devlin and co-workers[18] also observed increased contact ion pairing with increased temperature. They suggested that the

temperature effect is explained by "progressive partial desolvation" of the ions. Increased temperature forces solvent out of the ions' first coordination shells, which leads to an increase in the effective entropy of the solvent. Aqueous systems investigated by others[18,23,44–47] show the same general trends, with the solvent-separated pair minimum deeper due to the high dielectric constant of water. In more complicated solvents, there should be additional entropy considerations due to the librational and vibrational modes of the solvent. Increase in temperature favors the disruption of ion–solvent interactions in the drive to increase the total system entropy.

V. TRANSPORT PROPERTIES

Transport properties of interest were calculated through the use of sliding average methods. A typical simulation length for each system was 100 000 integration steps. The velocity autocorrelation function for species **a** is expressed as

$$\frac{\langle \mathbf{v}_A(t)\mathbf{v}_A(0)\rangle}{\langle \mathbf{v}_A(0)^2\rangle} \tag{10a}$$

and the current correlation function is expressed as

$$\frac{\langle \mathbf{j}(t)\mathbf{j}(0)\rangle}{\langle \mathbf{j}(0)^2\rangle}, \quad \text{where } \mathbf{j}=\sum_{i=1}^{\text{all ions}} q_i\mathbf{v}_i, \text{ respectively.} \tag{10b}$$

The self-diffusion coefficient D_a for species **a**, also known as the tracer diffusion coefficient, was calculated by two different methods. The first involves the integration of the velocity autocorrelation function by the equation

$$D_a = 1/3\int_0^\infty \langle \mathbf{v}_a(t)\mathbf{v}_a(0)\rangle dt. \tag{11a}$$

The second method uses the mean-squared displacement relation

$$2tD = \tfrac{1}{3}\langle \mathbf{r}^2(t)\rangle. \tag{11b}$$

Figure 9 gives a typical example of the behavior of the mean-squared displacement over time, in this case for systems A and B. While the mean-squared displacement of the small solvent is much larger than that expected for a relatively immobile polymer solvent,[48] structural properties of the electrolyte in a low molecular weight analog solvent can still be quite similar to those with a larger solvent.[7] The diffusion coefficients were calculated for the cation, anion, and solvent particles and are shown in Table III. It should be noted that the best statistics can be expected for simulations A through E, each of which lasted 100 000 time steps.

Figure 10 shows the velocity and current correlation functions obtained from simulation of system B at 270 K. Some insight into the behavior of systems at short times may be gained by frequency-dependent transforms of correlation functions. The frequency-dependent conductivity may be obtained from the current correlation function using the expression

$$\sigma(\omega)=\frac{1}{3Vk_BT}\int_0^\infty \langle \mathbf{j}(t)\mathbf{j}(0)\rangle e^{i\omega t}\,dt. \tag{12}$$

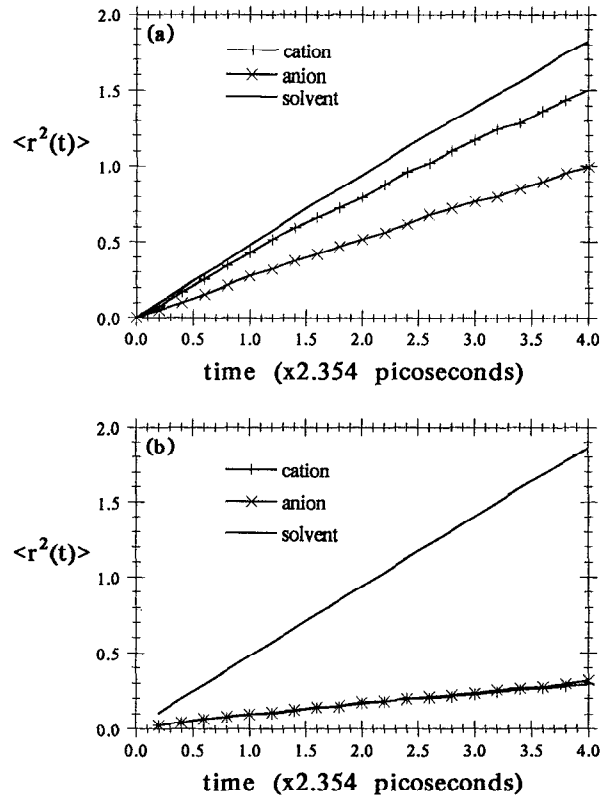

FIG. 9. Comparison of mean-squared displacements as a function of time at $T=270$ K, for system with (a) $z=1/2e$ and (b) $z=1e$, at an ion concentration of 1.8 M. (Experiments A and B.)

The value $\sigma(\omega=0)$ gives the direct-current (dc) conductivity. Figure 11 shows the frequency-dependent transforms for the current and velocity correlation functions in Fig. 10. Of special interest is the peak at approximately 240 cm^{-1} in the transform of the sodium velocity autocorrelation function. This maximum is believed to indicate the vibration of the sodium in its transitory cage of iodine and solvent particles. Our interpretation agrees with experimental data on the low-frequency vibrations found in sodium iodide solutions.[49]

A recent informative article based on both MD and analytical results[26] points out that increasing ion association in a system may be correlated with decreasing similarity between the velocity and current correlation functions due to the greater effect of cross correlations. The results for system B at 270 K in Fig. 10 show similar but not identical behavior for the cation and current correlation functions. This figure shows several distinct oscillations in the cation function, indicating that although significant ion association does exist, the cations are still mobile within their cage. In comparable simulations using a moment of inertia for the solvent 20 times larger than the one used here, the frequency-dependent conductivity is observed to show distinct peaks for ion motion within the cage and motion free of the cage.[26] With lower moments of inertia, the two channels are not separable.

Table IV presents the dc conductivities calculated by the method of Eq. (12). Also reported in the table are the calculated conductivities using the Nernst–Einstein relation, i.e., assuming that no pairing or clustering has occurred and the ions are moving independently. Comparison of the two dif-

TABLE III. Calculated diffusion coefficients.

Run	Temperature (K)	[From Eq. (11a)]$\times 10^{-9}$ m^2 s^{-1}			[From $\langle r^2(t)\rangle$]$\times 10^{-9}$ m^2 s^{-1}		
		D_+	D_-	D_s[a]	D_+	D_-	D_s[a]
A	180	1.27	1.07	1.76	1.02	0.85	1.65
	240	2.77	2.25	3.14	2.5	1.7	3.0
	315	3.68	2.14	3.8	...	...	...
	450	6.37	3.32	6.09	6.05	3	6.03
B	180	0.22	0.31	1.81	0.23	0.24	1.82
	270	0.5	0.62	3.42	0.49	0.53	3.10
	360	0.81	0.9	...	0.85	0.79	4.56
C	270	0.43	0.61	...	0.42	0.42	2.39
	360	0.44	0.52	4.13	0.35	0.34	3.93
D	360	1.05	1.35	4.82	1.16	1.17	4.89
E	360	0.68	0.85	4.32	0.66	0.69	4.14
G	270	0.55	0.92	3.45	0.68	0.84	3.46

[a]D for solvent particles.

ferent values for the conductivity by the equation[6]

$$\sigma=\frac{\frac{1}{2}Ne^2}{Vk_BT}(D_+ + D_-)(1-\Delta) \tag{13}$$

gives the value Δ, which is an indication of the degree of ion association in the system. The value for Δ varies from zero, which would indicate no ion association, to unity, which would indicate immobile ions and zero conductivity.

The value of Δ for a given system gives a quantitative indication of the degree to which ion association is affecting a given system's ability to transport ionic charge. The conclusions drawn earlier in this paper from structural properties are supported by the data discussed here. For example, ions in system A with charge $z=1/2$ appeared from the rdfs to move fairly freely from each other. The low values of Δ at all temperatures give the same indication. Doubling the charge to $z=1$ for system B results in a Δ close to unity. The mean-squared displacements for systems A and B shown in Fig. 9 illustrate the point further. In the system with $z=1/2$, the ions move at different rates, and the diffusion coefficient of the bulkier anion is greater than that of the cation. In the system with $z=1$, ion association has increased to the point that the ions move on average with the same diffusion coefficient.

The Δ value was studied by Boden *et al.* in concentrated polymer systems and was found to increase with increasing temperature and decreasing salt concentration. The values found were all high, indicating strong ion association.[6] On the other hand, molten salt systems in which current is believed to be carried by single ions were found to give Δ values between 0 and 0.16, where iodide salts gave smaller values and salts with smaller halides gave larger Δ values.[27] Our results agree with those of Boden showing that the Δ value decreases with higher salt concentration. The trend with regards to temperature is not so clear from the transport properties, but the structural properties discussed earlier clearly establish increased ion association with increasing temperature.

In an attempt to gain a microscopic picture of system behavior, ion coordinates were examined as a function of time. Significant clustering is clearly seen, as required by

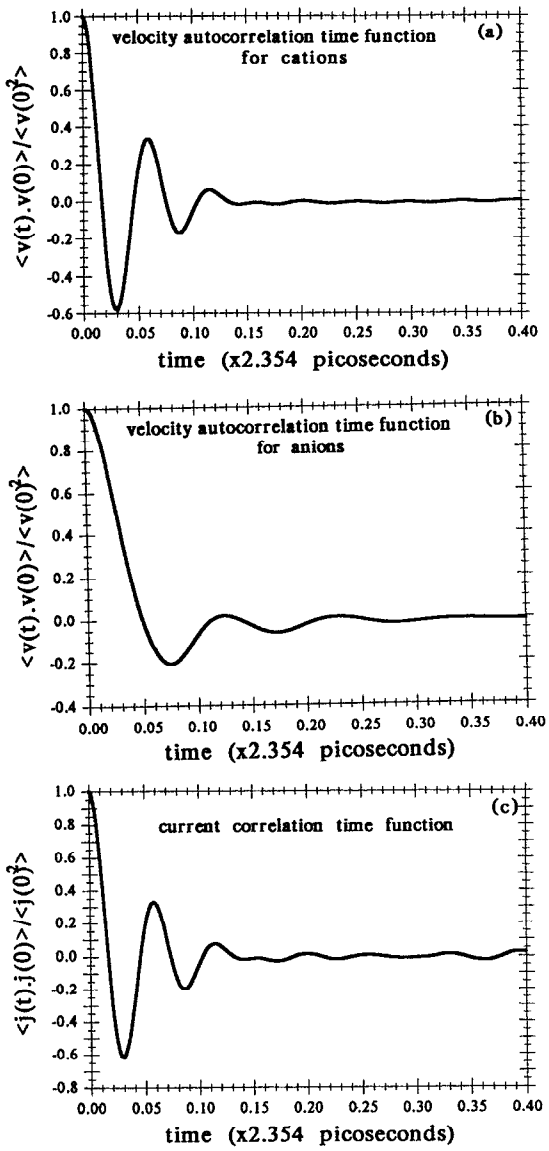

FIG. 10. Velocity autocorrelation functions for the cation and anion species at $T=270$ K, $z=1e$, and eight ion pairs. The current correlation function is also shown.

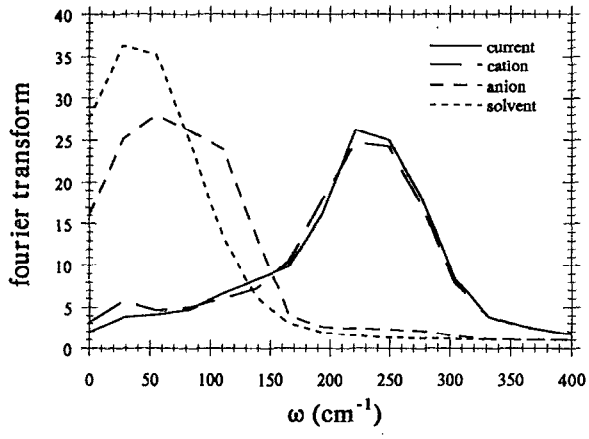

FIG. 11. Fourier transform of the correlation functions at $T=270$ K as a function of frequency for eight pairs with $z=1e$. The response of the current reflects that of the cation.

these stoichiometries. Within the time frame of these simulations, significant hopping of ions between clusters does not seem to occur, although rearrangement within and in the vicinity of clusters does. The MD work reported here suggests that ions in the NaI ether model system spend most of the time in clusters. However, it seems unlikely that large clusters actually conduct the current, since any moving cluster would encounter other clusters and change its identity. If some small, short-lived species exists and carries the current, it has not yet been observed in the simulation environment. Further work on this subject is underway.

VI. CONCLUSIONS

This paper presents a series of simulations aimed at elucidating the causes of phenomena common to polymer electrolytes and other systems of concentrated salts dissolved in polar, nonaqueous solvents. The structural and transport properties clearly establish significant ion association in systems where ion charge $z=1$. Ion clustering shows a strong increase with temperature. Thermodynamic analysis of the potential of mean force indicates that the temperature effect is driven by increase of entropy of the solvent, independent of whether the solvent is strong or weak dielectric.

TABLE IV. Conductivities and Nernst–Einstein corrections.

System	Temperature (K)	σ (S/m)	σ_{calc} (S/m)[a]	Δ[b]
A	180	4.64	5.22	0.11
	270	6.96	7.81	0.11
	450	8.88	10.1	0.12
B	180	0.72	5.24	0.86
	270	1.81	7.59	0.76
	360	1.64	9.15	0.82
C	270	4.45	12.5	0.64
	360	2.35	7.7	0.7
D	360	1.50	6.5	0.77
E	360	2.26	11.3	0.8
G	270	1.16	5.8	0.8

[a]Calculated from the Nernst–Einstein equation [Eq. (13) with $\Delta=0$].
[b]Defined in Eq. (13).

Examination of the microscopic behavior of the solvent indicates that in the systems with significant ion clustering, the ionic current is conducted by clusters; no direct evidence was found for ions hopping between clusters. In systems with relatively stronger ion–solvent interactions, such as those with $z=1/2$ or solvent dipole moment $\mu=2$ D, the ions are much freer, and ionic conductivity appears to be due to single ions. This trend is reflected in the lower values of the correlation factor Δ. The actual effect of varying concentration on ionic conductivity, however, seems dominated by the reduction in the individual ionic diffusion coefficients with increased charge density.

ACKNOWLEDGMENTS

This work was supported by the NSF/MRC through the Northwestern MRL, Grant No. DMR 9120571, and by the ARO DAAL-03-90-G-0044. Supercomputer support was provided by the Pittsburgh Supercomputer Center, Grant No. DMR910014P. M. F. and V. A. P. gratefully acknowledge a Fulbright Postdoctoral Fellowship and an NSF Graduate Fellowship, respectively. We are grateful to S. D. Druger, A. Nitzan, M. Lonergan, and J. W. Perram for incisive discussions; and to M. D. Todd for graphical advice.

[1] F. M. Gray, *Polymeric Solid Electrolytes* (VCH, New York, 1991).
[2] R. A. Robinson and R. H. Stokes, *Electrolyte Solutions*, 2nd ed. (Butterworths, London, 1968), Chaps. 4 and 14.
[3] S. I. Smedley, *The Interpretation of Ionic Conductivity in Liquids* (Plenum, New York, 1980), Chap. 2.
[4] F. Accascina and R. M. Fuoss, *Electrolytic Conductance* (Wiley, New York, 1959).
[5] *Physics of Superionic Conductors*, edited by J. W. Perram (Plenum, London, 1983).
[6] N. Boden, S. A. Leng, and I. M. Ward, Solid State Ionics **45**, 261 (1991).
[7] J. R. MacCallum, A. S. Tomlin, and C. A. Vincent, Eur. Polym. J. **22**, 787 (1986).
[8] M. C. Wintersgill, J. J. Fontanella, S. G. Greenbaum, and K. J. Adamić, Br. Polym. J. **20**, 195 (1988).
[9] C. W. Davies, *Ion Association* (Butterworths, London, 1962), Chap. 10.
[10] J. Ludwig, K. Duppen, and K. Kommandeur, J. Chem. Soc. Faraday Trans. 1 **80**, 2943 (1984).
[11] H. Cheradame, in *IUPAC Macromolecules*, edited by H. Benoit and P. Rempp (Pergamon, New York, 1982), p. 351.
[12] M. Kakihana, S. Schantz, and L. M. Torell, J. Chem. Phys. **92**, 6271 (1990); S. Schantz, L. M. Torell, and J. R. Stevens, *ibid.* **94**, 6862 (1991).
[13] S. Schantz, Ph.D. thesis, University of Gothenburg, 1990.
[14] D. E. Irish and M. H. Brooker, Adv. Infrared Raman Spectrosc. **2**, 212 (1976).
[15] B. L. Papke, M. A. Ratner, and D. F. Shriver, J. Electrochem. Soc. **129**, 1694 (1982); J. Phys. Chem. Solids **42**, 493 (1981).
[16] D. N. Bhattacharyya, C. L. Lee, J. Smid, and M. Szwarc, J. Phys. Chem. **69**, 608 (1965).
[17] C. Carvajal, K. J. Tölle, J. Smid, and M. Szwarc, J. Am. Chem. Soc. **87**, 5548 (1965); W. Y. Xu, J. Smid, and M. Van Beyelen, Solid State Ion. **57**, 133 (1992).
[18] R. Wooldridge, M. Fisher, G. Ritzhaupt, and J. P. Devlin, J. Chem. Phys. **86**, 4391 (1987).
[19] D. Teeters and R. Frech, Solid State Ion. **18/19**, 271 (1986).
[20] M. A. Ratner and A. Nitzan, Faraday Discuss. Chem. Soc. **88**, 19 (1989).
[21] R. Olender and A. Nitzan, Electrochim. Acta **37**, 1505 (1992); J. Chem. Phys. (submitted).
[22] W. L. Jorgensen, Adv. Chem. Phys. **70**, 469 (1988); J. K. Buckner and W. L. Jorgensen, J. Am. Chem. Soc. **111**, 2507 (1989).
[23] O. A. Karim and J. A. McCammon, J. Am. Chem. Soc. **108**, 1762 (1986); M. Berkowitz and W. Wan, J. Chem. Phys. **86**, 376 (1987); A. C. Belch,

M. Berkowitz, and J. A. McCammon, J. Am. Chem. Soc. **108**, 1755 (1986).
[24] P. Bopp, I. Okada, H. Ohtaki, and K. Heinzinger, Z. Naturforsch. Teil A **40**, 116 (1985); W. Meier, P. Bopp, M. M. Probst, E. Spohr, and J.-I. Lin, J. Phys. Chem. **94**, 4672 (1990).
[25] S.-B. Zhu and G. W. Robinson, Z. Naturforsch. Teil A **46**, 221 (1990).
[26] A. Chandra, D. Wei, and G. N. Patey, J. Chem. Phys. **99**, 2083 (1993).
[27] G. Ciccotti, G. Jacucci, and I. R. McDonald, Phys. Rev. A **13**, 426 (1976).
[28] J. Perkyns and B. M. Pettitt, J. Chem. Phys. **97**, 7656 (1992).
[29] V. Vlachy, T. Ichiye, and A. J. Haymet, J. Am. Chem. Soc. **113**, 1071 (1991).
[30] H. J. Friedman, Annu. Rev. Phys. Chem. **32**, 179 (1981).
[31] J. M. Caillol, D. Levesque, and J. J. Weis, J. Chem. Phys. **91**, 5544, 5555 (1989); J. M. Caillol, D. Levesque, J. J. Weis, G. N. Patey, and P. G. Kusalik, Mol. Phys. **62**, 461 (1987); J. M. Caillol, D. Levesque, and J. J. Weis, J. Chem. Phys. **85**, 6645 (1986).
[32] J. Eggebrecht and P. Ozler, J. Chem. Phys. **93**, 2004 (1990); J. Eggebrecht and G. H. Peters, *ibid.* **93**, 1539 (1993).
[33] L. R. Zhang, H. S. White, and H. T. Davis (unpublished).
[34] S. F. Mills and C. R. A. Catlow, Solid State Ion. (to be published); S. Neyertz and J. Thomas, *ibid.* (to be published).
[35] W. L. Jorgensen and M. Ibrahim, J. Am. Chem. Soc. **103**, 3976 (1981).
[36] S. W. de Leeuw, J. W. Perram, and E. R. Smith, Annu. Rev. Phys. Chem. **37**, 245 (1986); S. W. de Leeuw, B. Smit, and C. P. Williams, J. Chem. Phys. **93**, 2704 (1990).
[37] S. Nosé, Mol. Phys. **52**, 255 (1984).
[38] A preliminary version of some of the current results has been published as M. Forsyth, V. A. Payne, M. A. Ratner, S. W. de Leeuw, and D. F. Shriver, Solid State Ion. **53–56**, 1011 (1992).
[39] T. E. Hogen-Esch and J. Smid, J. Am. Chem. Soc. **88**, 318 (1966).
[40] L. L. Chan, K. H. Wong, and J. Smid, J. Am. Chem. Soc. **92**, 1955 (1970).
[41] G. J. Janz and R. P. T. Tomkins, *Nonaqueous Electrolytes Handbook* (Academic, New York, 1973), Vol. 2, Chap. 1.
[42] Y. Marcus, *Ion Solvation* (Wiley, New York, 1985), Chap. 8.
[43] B. M. Pettitt and P. J. Rossky, J. Chem. Phys. **84**, 5836 (1986).
[44] L. X. Dang, J. Chem. Phys. **97**, 1919 (1992).
[45] S. E. Huston and P. J. Rossky, J. Phys. Chem. **93**, 7888 (1989); S. W. Chen and P. J. Rossky, *ibid.* **97**, 6078 (1993).
[46] G. Ciccotti, M. Ferrario, J. T. Hynes, and R. Kapral, J. Chem. Phys. **93**, 7137 (1990).
[47] D. E. Smith, L. Zhang, and A. D. J. Haymet, J. Am. Chem. Soc. **114**, 5875 (1992).
[48] P. G. Bruce and C. A. Vincent, Faraday Discuss. Chem. Soc. **88**, 43 (1989); M. Armand, *ibid.* **88**, 65 (1989).
[49] B. Guillot, P. Marteau, and J. Obriot, J. Chem. Phys. **93**, 6148 (1990).